



## A recent tactic for searching CDK-7 kinase inhibitor by NCI database screening

MOHAMMAD RASHID<sup>1\*</sup>, MD TANWIR ATHAR<sup>1</sup>, AFZAL HUSSAIN<sup>2</sup>, NORAH M. ALMADANI<sup>3</sup> and ASHFAQ HUSSAIN<sup>4</sup>

<sup>1</sup>Department of Pharmacognosy and Pharmaceutical Chemistry, College of Dentistry and Pharmacy, Buraydah Private Colleges, Buraydah-51418, Saudi Arabia, <sup>2</sup>Department of Bioinformatics, Maulana Azad National Institute of Technology Bhopal, Madhya Pradesh-462003, India, <sup>3</sup>Biochemistry Department, Faculty of Science, University of Tabuk, Tabuk-47914, Saudi Arabia and <sup>4</sup>Department of Electronics Engineering, Rajasthan Technical University, Kota-324010, India

(Received 26 June, revised 9 August, accepted 21 October 2023)

**Abstract:** The present study was based on an exploration of NCI database for searching specific CDK-7 kinase inhibitor by HTVS, SP, XP, molecular docking, molecular dynamic simulation, and ADMET evaluation. The best CDK-7 kinase inhibitors (NCI613391, NCI169676, NCI281246, NCI339580) were identified via NCI database screening. The stability of binding interaction between receptor protein and protein-ligand complex of potent finding compounds (NCI613391) was further confirmed by dynamics simulations and MM-GBSA. The RMSD value of receptor and receptor–ligand complexes was analysed, and it revealed the stability of binding interactions and remained stable throughout the simulation. The RMSF values and gyration radius of the unbound receptor and backbone atoms of the complex were found to be equal, which indicates that the drug molecule inside the CDK7 receptor is also stable. The study of MM-GBSA data also revealed stronger binding interactions of ligands to CDK7 receptors. With the exception of NCI169676, all compounds were shown to be substrates for CYP450 2D6, CYP450 3A4, inhibitors of CYP450 2C9, and non-inhibitors of p-glycoprotein. All compounds were qualified and found suitable to be as drug-likeness according to the Lipinski rule, Ghose filter, MDDR like rule and CMC-like rule. The compound (NCI613391) exhibited human intestinal absorption (76.08%), displayed negative AMES and T.E.S.T (US-EPA) toxicity with OSIRIS property and found to be a promising CDK-7 kinase inhibitor and its efficacy may be further explored in clinical trials.

**Keywords:** NCI database; CDK-7 kinase inhibitor; dynamic simulation; molecular docking; T.E.S.T (US-EPA); Lipinski's rule; OSIRIS property.

\* Corresponding author. E-mail: Rashid.Mohd@bpc.edu.sa; rashidpharm2008@gmail.com  
<https://doi.org/10.2298/JSC230624083R>

## INTRODUCTION

Cancer is a word for a condition in which cells divide *via* mitosis without regulation of the cell cycle (uncontrolled cell growth), hence cell cycle is a well-known feature of cancer's foundation.<sup>1</sup> Cyclin-dependent kinase-7 (CDK7) protein levels are raised in many forms of cancer cells, and cell development is also dependent on CDK7 activity in comparison to normal tissues, and thus it's a source of clinical conditions. Many types of cancer cells have elevated amounts of the protein cyclin-dependent kinase-7 (CDK7), and in contrast to normal tissues, CDK7 activity is required for cell development, which is a source of clinical consequences.<sup>2</sup> These results suggest that cyclin-dependent kinase-7 inhibitors (CDK7i) may represent a promising therapeutic target for cancer, and recent papers have emphasized the critical role of CDK7i in the development of many cancer types.<sup>3,4</sup>

A cyclin-dependent protein kinase called cyclin-dependent kinase-7 (CDK7) regulates cell cycle progression by phosphorylating to other CDKs and altering their activity. The ability of cyclin-dependent kinase-7 inhibitors (CDK7i) to overcome the resistance to cancer treatments and to stop the cell cycle, induce apoptosis, and suppress transcription, particularly of super enhancer-associated genes in cancer, has also been demonstrated in preclinical research. For these reasons, the authors selected CDK7i as a potent therapeutic target. Due to its simultaneous involvement in regulating the cell cycle and modulating transcription, cyclin-dependent kinase-7 (CDK7) has been investigated as an anticancer therapeutic target and numerous CDK7 selective inhibitors have been developed and tried as cancer therapies.<sup>5,6</sup> For the treatment of advanced solid tumours, four selective CDK7 inhibitors (ICEC0942, SY-1365, SY-5609 and LY340515) have recently advanced to Phase I/II clinical trials. These studies also showed that CDK7i has the ability to overcome cancer therapy resistance (for details see Supplementary material to this paper).

The National Cancer Institute (NCI) of the National Institutes of Health, United States of America, is the world-oriented organization for searching and developing novel potent therapeutic agents for fighting with multiple types of cancer cells.<sup>7,8</sup> That's why authors choose NCI databases as repurposing for searching for new molecules as potent and specific CDK7 inhibitors by SBVS followed by molecular dynamics (MD) simulations and MM/GBSA evaluation to know the ligand-receptor binding interaction and to establish the stability in the binding pocket of receptor.<sup>9,10</sup> Lack of knowledge on ADMET, drug similarity, drug score, and bioactivity profile are the main causes of drug failure during the development stages. Thus, the authors also predicted the physiochemical characteristic, ADMET, drug score and bioactivity profile by Molinspiration, Pre-ADMET prediction, Osiris property explorer and T.E.S.T. (US-EPA).

## EXPERIMENTAL

### *Protein structure preparation and selection*

The cyclin-dependent kinase 7 (CDK-7) protein was retrieved and obtained from the Protein Data Bank (PDB ID: 1UA2), in addition to being generated using the protein production tool in the Maestro Schrodinger software (<https://www.rcsb.org/structure/1ua2>). The constructed protein was given bonding instructions, the hydrogen atoms were integrated, and the structure was subjected to energy minimization using an OPLS-2005 force field with an energy cutoff value of 0.30 Å for root mean square deviation (RMSD).<sup>11</sup>

### *National Cancer Institute (NCI) Database Compounds and reference ligand preparation*

The NIH-NCI (National Institutes of Health-National Cancer Institute, USA) release database was used to collect the molecular series (database). (<https://cactus.nci.nih.gov/ncicadd/about.html>, 2022). The ligand was then prepared using Schrödinger software's LigPrep module.<sup>12</sup>

### *Preparation of the grid*

The receptor grid generation panel and glide framework were used to generate the grid of the prepared target protein (CDK7). For CDK7, the adenosine triphosphate (ATP) molecule was selected eccentrically. With the partial charge cutoff set to 0.25, the scaling factor was set to 1.0.<sup>13</sup>

### *Molecular docking and screening*

Structure-based virtual screening (SBVS) uses a computer approach known as molecular docking to anticipate how ligands (drug-like small molecules) would interact with a target receptor's binding site, which is often a protein structure.<sup>14</sup> To get best result, high-throughput virtual screening (HTVS), standard precision (SP), extra precision (XP) docking was employed, and XP descriptors information was also picked for pose viewing.

### *Analysis of drug-like characteristics*

Screened National Cancer Institute (NCI) compounds were chosen for the drug-like property assessment. These properties were subject to Lipinski's rule of five. Molecular weight (MW), hydrogen bond acceptor (HBA), total solvent accessible surface area (SASA), human oral absorption (HIA), hydrogen bond donor (HBD) and predicted aqueous solubility (*QPlogS*) were among the parameters collected. The Pfizer rule implicitly states that a medicine must have a balanced hydrophilic-lipophilic nature.<sup>15</sup>

### *MM/GBSA evaluation method for drug-target binding energy analysis*

The drug-target binding energy was calculated by using the MM/GBSA method of Schrodinger software. The stability of target protein and ligand complexes is determined using this binding energy calculation.<sup>16</sup>

### *Simulation of molecular dynamics (MD)*

A computer simulation technique for analysing the physical motions of atoms and molecules is called molecular dynamics (MD). For a predetermined period of time, the atoms and molecules are permitted to come into contact, giving insight into the dynamic evolution of the system. In addition to the protein structure of CDK7 Kinase (PDB code 1UA2), the top three docked complexes, NCI613391 (-13.063 kJ/mol) was subjected to 200 ns MD simulations utilizing the CHARMM27 all-atom force field using Gromacs 2021.3 software (<http://www.gromacs.org>).<sup>17</sup> The protonation state was checked by using GROMACS pdb2gmx program and missing hydrogens were added. The parameters for the ligand coordinates and

topology were obtained using the Swiss param.  $\text{Na}^+$  and  $\text{Cl}^-$  were used to do the neutralization process, and the TIP3P water cube model was used to perform the solvation ([https://en.wikipedia.org/wiki/Molecular\\_dynamics](https://en.wikipedia.org/wiki/Molecular_dynamics), 2022).<sup>18-19</sup>

#### *Lipinski's rule and drug similitude*

When a ligand molecule violates the Lipinski rule of 5, which is when it has more than five hydrogen bond donors, a molecular weight greater than 500, a  $\log P$  value greater than 5, and a total of N and O greater than 10, poor absorption or penetration is much more likely to happen.<sup>20</sup> To assess whether a particular molecule is similar to well-known drugs, numerous chemical features and attributes must be carefully balanced.<sup>21</sup>

#### *Prediction of drug-likeness characteristics*

The Pre ADMET program's tool forecasts drug-like features based on Lipinski's rule in addition to other well-known rules such the Ghose filter,<sup>22</sup> CMC,<sup>23</sup> WDI<sup>24</sup> and MDDR.<sup>25,26</sup> These laws acted as filters, separating chemicals with drug-like properties from those without. The Ghose filter uses the following factors to predict the drug-likeness: molecular weight between 160 and 480, molar refractivity between 40 and 130, predicted  $\log P$  in between -0.4 and 5.6, and the total number of atoms between 20 and 70 (for details see Supplementary material).<sup>26,27</sup>

#### *A Molinspiration algorithm for predicting drug similarity*

Molinspiration (2018.02 version) was used to add a SMILES representation of the NCI-screened compounds in order to predict drug-like characteristics and bioactivity scores against drug targets like enzymes, nuclear receptors, GPCR ligands and ion channel modulators (<https://www.molinspiration.com/cgi/properties>). The SMILES representation was created using the Chem. Bio draw Ultra software (11.0 versions). To determine the percentage of absorption, the formula  $\% \text{Ab} = 109 - (0.345 \text{TPSA})$  was employed (for details see Supplementary material).<sup>26,27</sup>

#### *Examining Osiris's potential as a drug and its relevant properties*

It was developed by T. Sander and used for the first time at Actelion Pharmaceuticals Ltd. as a part of the compound registration system in the drug development division. It is used to determine pharmacokinetic parameters such as toxicity potential, solubility, overall drug-likeness and drug score of compounds ([www.organicchemistry.org/prog/peo/](http://www.organicchemistry.org/prog/peo/), for details see Supplementary material).<sup>26,28</sup>

#### *Acute toxicity prediction by Pre ADMET program and T.E.S.T. tool*

The acute toxicity was anticipated using the mutagenicity of Ames test (<https://preadmet.bmdrc.kr/toxicity/>) and the T.E.S.T. tool (version 4.2.1), a US Environmental Protection Agency program (<https://www.epa.gov/chemical-research/toxicity-estimation-software-tool-test>).<sup>27,29,30</sup> Dr. Ames developed the straightforward Ames test to determine whether a material is mutagenic or not. It uses several strains of the bacterium *Salmonella typhimurium*, which needs histidine to develop due to the gene changes in histidine production (for details see Supplementary material).<sup>31-34</sup>

## RESULTS AND DISCUSSION

#### *Target protein docking score and analysis*

In order to examine the potential for NCI selected top drug-like compounds to be involved in the CDK7 kinase binding pocket, the molecular docking simul-

ations were carried out. The results of energies and various interactions with the residues of the amino acids in the CDK7 binding pocket are listed in Tables I and S-II of the Supplementary material. Four hydrogen bonds were found to exist between NCI613391 and GLU20, THR170, MET94, and GLU95 (2.15, 1.43, 2.30 and 1.68 Å, respectively). Four hydrogen bonds were found in NCI613391, including one with MET94 (2.30 Å), thought to be crucial for the action and others with GLU20 (2.15 Å), THR170 (1.43 Å), and GLU95 (1.68 Å). Table S-I show the docking rating and binding interaction of NCI-screened compounds with the target protein's active site residues (see Supplementary material). The NCI-screened molecular docking and their Lig plot chart interaction diagram demonstrates the interaction discovered with the target protein of top scored score and is displayed in Figs. 1 and S-2 (Supplementary material).

TABLE I. The molecular docking analysis of NCI ten best finding compounds against the residue protein of CDK7 kinase;  $E_b$  – free binding energy; H-bond – number of H-bonds; residues – interacting residues

Compd. ID	H-Bonding interactions				Hydrophobic interaction and salt bridge	
	$E_b$ kJ/mol	H-bonds	Residue	distance Å	Tot. Numb.	Residue
NCI613391	-73.25	4	GLU20 THR170 MET94 GLU95	2.15, 1.43, 2.30, 1.68	7	LEU18, ALA39, PHE91, PHE93, MET94, VAL100, LEU144
NCI169676	-64.36	2	GLU20 THR170	1.85, 1.72	7	VAL100, LEU18, MET94, PHE93, PHE91, ALA39, LEU144
NCI281246	-53.57	2	GLU95 MET94	1.86, 2.08	7	LEU18, VAL26, MET94, PHE93, PHE91, ALA39, LEU144
NCI339580	-59.83	4	LEU18 GLU99 MET94 THR170	2.41, 2.13, 2.11, 1.74	7	LEU18, MET94, PHE93, PHE91, ALA39, LEU144, VAL26

#### *Drug-likeness properties and ADME/T analysis of best NCI screened compounds*

All of the NCI-screened compounds were found to have oral absorption within the range of the human oral absorption limit, which is between 36.306 and 73.745 (25 % less and >80 % high). Compound NCI169676 was found to have high oral absorption (73.745) and molecular weights also to be under the limit of 500 Da. The aqueous solubility ( $QPlogS$ ) of all investigated compounds was found to be within the acceptable range (-6.5 to 0.5) with values ranging from -1.162 to -3.246 and hydrogen bond donor (HBD) count in between 2 and 4,

which is below the permitted limit ( $\leq 5$ ). The number of hydrogen bond acceptor (*HBA*) of all compounds was also observed under permissible limit ( $\leq 10$ ) that is in between 6 and 9 (Table S-III of the Supplementary material).

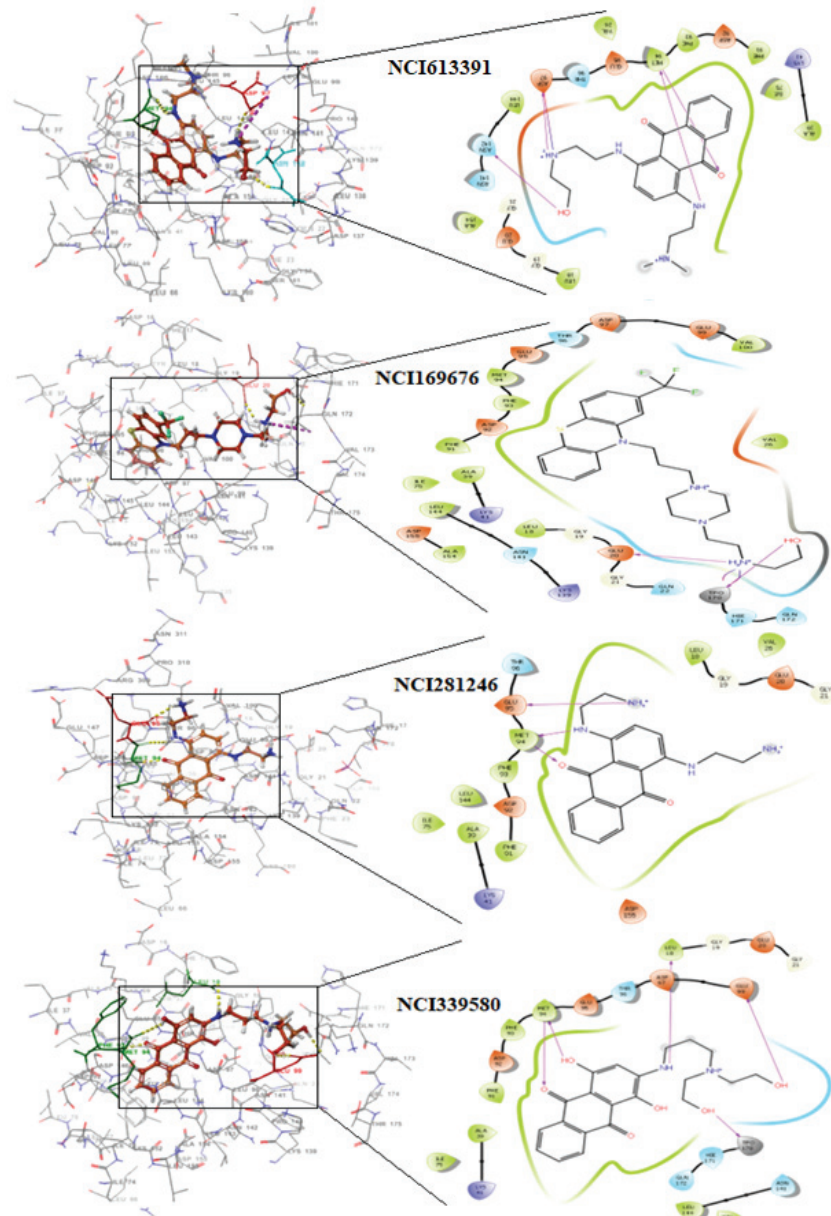


Fig. 1. NCI docking scores molecule binding interaction diagram and corresponding lig-plot interaction diagram by docking analysis in the active site residues of CDK7 kinase protein.

The *SASA* of NCI-screened compounds was found to be between 604 and 832 under the limit (300–1000) in the current investigation, indicating good oral bioavailability (Table S-III and Fig. S-3 of the Supplementary material). Additionally, the skin permeability (*QPlogPw*) of compounds subjected to NCI screening was found to be in between 12 and 17, within the permissible range (4.0–45.0). *QPplorz* was in the range of 32.904–47.868 (permissible scale: 13.0–70.0), *QPlogPoct* in the range of 19.887–26.284 (permitted scale: 8.0–35.0), *QPlogPo/w* in the range of 0.8–3.729 (permitted scales: –2.0–6.5) and *QPlogPC16* within the range of 11.341–16.161 (permitted scales: 4.0–18.0). Skin permeability in form of *QPlogPw* (permitted scale: 4.0–45.0) and binding to human serum albumin in form of *QPlogKp* (permitted scale: –8.0 to 1.0) were observed in the acceptable ranges of 12.183–17.178 and –5.387 to –7.577, respectively. In the range of –0.064 to 0.576 independent aqueous solubility in the form of *QPlogKhsa* was also observed within the permissible limit (–1.5 to 1.5) (Table S-IV of the Supplementary material).

#### *Prime MM/GBSA module for drug-target binding energy assessment*

The NCI compounds that were screened, specifically NCI613391 (complex with PDB ID: 1UA2), exhibit a high amount of binding free energy (*G bind* = = –73.25 kJ/mol). Among all the molecules, the ligand (NCI613391) complex had the largest negative binding free energy (–73.25 kJ/mol), while NCI281246 had the lowest (–53.57 kJ/mol). Despite having a higher hydrogen occupancy than other compounds, compound NCI613391 complex shows a more stable engagement in the active free binding site of receptor. Since the NCI281246 complex has the lowest free binding energy, its interaction with the CDK7 active site during binding is the weakest. Surprisingly, the compound NCI613391 was found to have superior binding affinity to the CDK7 receptor binding site when compared to other substances. The compounds  $\Delta G$  values were further broken down into their component parts, which are shown in Table S-V and Fig. S-4 (Supplementary material).

#### *Structural analysis of NCI screened ligands by molecular dynamic simulation (MD)*

In the ATP binding pocket, the ligand NCI NCI613391 interacts with GLU20, THR170, MET94 and GLU95 via stable hydrogen bonds with distances of 2.15, 1.43, 2.30 and 1.68 Å, respectively. NCI613391 had the highest docking score (–13.06 kJ/mol), and 63 % of its bonds were H-bonds. The ligand NCI613391's amide moiety (N-terminal) joins MET94 through its C-terminal in a strong H-bond. Because of the binding linker (residue) that is primarily conserved on the protein's alpha helix (GLU20 & THR170) and coil (MET94 & GLU95), the secondary structure of CDK7's alpha helix and coil was made to

stabilize hydrogen bonding more. LEU18, ALA39, PHE91, PHE93, MET94, VAL100 and LEU144 all showed interactions with the hydrophobic benzene pie ( $\pi$ ). The NCI NCI613391 molecule has the largest percentage of H-bonds among the compounds, and its H-bonding network appears to be fairly stable in the *RMSD*, *RMSF* and radius of gyration (*Rg*, Fig. 2A).

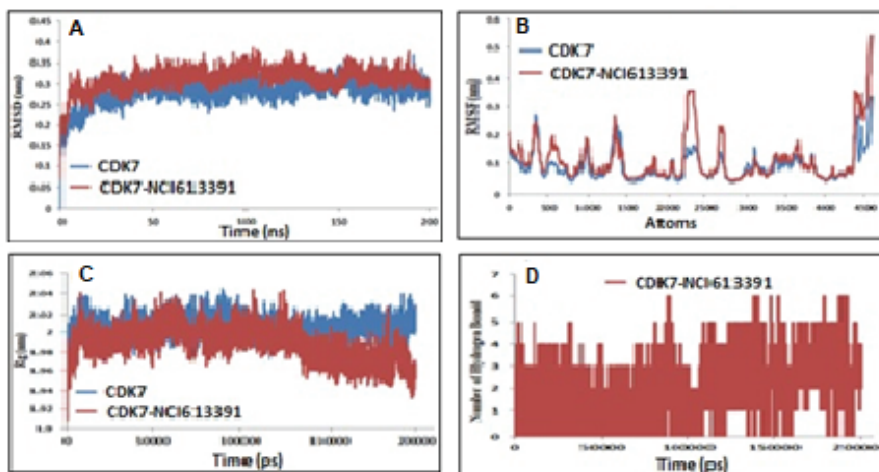


Fig. 2. MD simulation trajectory plot of CDK7 receptor protein backbone over a time period of 200 ns with NCI screened HIT molecules. A: the *RMSD* of NCI613391. B: the *RMSF* of the NCI613391. C: the *Rg* of the NCI613391. D: the hydrogen bond analyses of the NCI613391.

How much a protein changes when its primary coordinates are altered is determined by the *RMSD* score. Following a start time of 15 ns in the given MD simulation, the investigated ligand-receptor targets showed effective conversion. In terms of their backbone, the obtained complex *RMSD* trajectories rise throughout the first frames until the *RMSDs* level off at about 20 ns, at which point the subsequent trajectories continued around the corresponding average values until 200 ns in the case of the ligand (NCI613391). Through the course of the MD simulation, the latter differential dynamic behaviour grants NCI613391 a more stable and confinement-friendly environment inside the CDK7 kinase binding site. The ligand (NCI613391) extends to the ATP binding site to gain additional strength thanks to the four hydrogen bonds and the highest hydrogen bond occurrence percentage. In addition, the ligand has extensive VdW interactions with the seven nearby residues (LEU18, ALA39, PHE91, PHE93, MET94, VAL100 and LEU144). Throughout the simulation, the stability profile of NCI-screened drug in association with the CDK7 kinase was monitored using the GROMACS command line `gmx_rmsd` to calculate the *RMSD* values.

Additionally, the ligands showing significant *RMSD* values for their specific ligand–protein complexes would indicate insufficient ligand accommodation within the examined pocket across the chosen MD simulation time-frames. Using the initial structure as a frame of reference (0 to 200 ns), the *RMSD* values for the protein backbone and possible inhibitors were evaluated. The *RMSDs* of the free CDK7 kinase receptor and CDK7+NCI613391 complexes are shown in Fig. 2A. While the *RMSD* values of the analysed parameters for the complexes CDK7+NCI613391 gradually increased from 0 to 50 ns and remained stable after equilibration during simulation duration, the complex CDK7+NCI613391 was discovered to be equal to the receptor CDK7 Kinase protein.

The NCI screened for ligand-bound protein relative to the CDK7 kinase to calculate the residue root-mean-square fluctuation (*RMSF*) in order to get further understanding of the stability of the ligand binding complex. Using the GROMACS “gmx rmsf” command line, the individual backbone *RMSF* of each protein was calculated. This flexibility validation criterion was developed to offer information on the contribution of specific protein residues to structural fluctuations in the ligand–protein complex. In the reduced beginning structures, *RMSF* calculates the average deviation over time for each residue from its reference position. The backbone atoms’ *RMSF* value was calculated, and the *RMSF* figure shows (Fig. 2B) that the fluctuations are on an atom-scale. The CDK7 kinase protein complexes (CDK7+NCI613391) were discovered to have low *RMSF* values and the atoms’ fluctuations data was found to be essentially equal to that of the free receptor. As a result, the *RMSF* plot showed that the binding interactions of all the tested medications were shown to be stable within the receptors and that the simulation analysis study had no appreciable impact on the receptor’s flexibility.

*Rg* was applied throughout the entire MD trajectories by GROMACS “gmx\_gyrate” command script in order to learn more about the stability of the ligand complex. The *Rg*, which is calculated during molecular simulation, is also used to determine how compact a protein is; if the protein is particularly compact, it will not fold readily and the complex will be stable in both folded and unfolded states. The distance between all scattering components and the molecular centre of mass is measured as the radius of gyration, which is widely used to reflect structural changes in a substance. The CDK7 kinase receptor and CDK7+NCI613391 complexes was all identified by the *Rg* plot as having similar properties. As shown in Fig. 2C, the *Rg* values of protein and protein–drug candidate complexes showed a striking similarity and a stable folded structure to the protein complex. The *Rg* values from the current investigation support NCI613391–CDK7 complex’s improved stability. The ligand (NCI613391) complex was discovered to have low and average *Rg* values, which point to the ligand’s compactness and stability in CDK7 kinase binding site.

In NCI613391, four hydrogen bonds were observed, one with MET94 (2.30 Å) which is assumed to be essential for the activity and another with GLU20 (2.15 Å), THR170 (1.43 Å) and GLU95 (1.68 Å). Two hydrogen bonds were observed for NCI122039, one of them with GLU95 (1.85 Å) and another with MET94 (1.81 Å) which is assumed to be essential for the activity. For compound NCI196464, one hydrogen bond was observed with MET94 which is assumed to be essential for the activity. The more H-bonding and its occupancy at the active binding site of receptor, directs the more stability of complex. More stable complex of compounds NCI613391 contains four H-bond with GLU20, THR170, MET94 and GLU95 (60 % H-bond occupancy, Fig. 2D). In the entire simulation, the ligand (NCI613391) showed the highest hydrogen bond occupancy with CDK7 residues protein.

#### *The physicochemical properties prediction*

Interestingly, the molecular weight of NCI-screened compounds was found in the range of 297.17–426.79 (under the Lipinski limit), which is less than 500 and easily transported, diffused and absorbed in comparison to heavy molecules. The number of hydrogen bond acceptors (*n*-ON, O and N atoms) was found within the Lipinski limit range, which is less than 10. The number of hydrogen bond donors (*n*-OHNH, NH and OH) of compounds were also found to be within the Lipinski limit range, that is, less than 5, except for compounds NCI613391 and NCI281246 (six donors were found). The lipophilicity of compounds was also found to be within a range limit that is less than 5, which is an indication for good lipid solubility that will help the drug interact with membranes. As the number of rotatable bonds increases, the molecule becomes more flexible and adaptable for efficient interaction with a particular binding pocket. Remarkably, all compounds were found to have rotatable bonds within range limits 2–10, except the compound NCI613391, which was flexible within the Lipinski limit (Table S-VI of the Supplementary material). The *TPSA* was calculated from the surface areas that are occupied by oxygen and nitrogen atoms and hydrogen atoms attached to them, thus it is closely related to the hydrogen bonding potential of compounds (Table S-VII of the Supplementary material).

#### *The score of bioactivity*

The compound NCI613391 was found to have better ligands for protease inhibitors, nuclear receptor ligands, GPCR ligands, kinase inhibitors, enzyme inhibitors, ion channel modulators and nuclear receptor ligands (Table S-VIII of the Supplementary material).

#### *The Osiris property explorer*

The obtained results clearly showed that the compound NCI613391, which showed green colour with the tumorigenic effect and the reproductive effect

would be safe. All the tested compounds showed green colour indication with the tumorigenic effect except NCI339580 and the reproductive effect except NCI169676. Most of the compounds were observed to have an irritant effect, except NCI169676 (Table S-IX of the Supplementary material).

#### *The prediction of ADME/T properties by pre-ADMET server*

All compounds displayed negative carcinogenicity in rats as well as mice, except compounds NCI294726 (Table S-X of the Supplementary material). The obtained result from the pre-ADMET server revealed that the compounds NCI169676 showed high human intestinal absorption (HIA) scores of more than 90 % in comparison to other compounds. The compounds NCI613391, NCI281246 and NCI339580 were observed to have a better human intestinal absorption (HIA) score. All of the compounds were found to have a low value of blood-brain barrier (BBB) penetration (<1). The skin permeability value in cm/h ( $\log K_p$ ) was also found within the limit range of NCI screened compounds (Table S-XI of the Supplementary material).

#### *The acute toxicity prediction by T.E.S.T. (US-EPA) web-based server*

The hierarchical clustering method predicted an oral rat LD<sub>50</sub> in the range of 1.94–2.36 (–Log 10, mol/kg). The consensus approach, hierarchical clustering, FDA and nearest neighbour determined that the drugs' mutagenic values fell within the ranges of 0.53–0.95, 0.66–0.81, 0.53–0.97 and 0.33–0.67 mol/kg, whereas the FDA method and the nearest neighbour technique and other toxicity outcomes are shown in Table S-XII (Supplementary material).

#### *The Prediction of metabolism by pre-ADMET web server*

All the compounds showed inhibition of CYP450-2C9 except NCI169676. Regarding the substrate of CYP450-3A4, all the compounds exhibited as substrates except the compound NCI169676 (non-substrate). All of the NCI screened compounds were found to be non-inhibitors of p-glycoprotein, except the compound NCI169676 (Table S-XIII of the Supplementary material).

#### *Drug likeness and rule violation prediction of NCI screened compounds*

Drug-like characteristics of NCI-screened compounds were estimated by various drug-like rules, like Lipinski's rule, the Ghose filter, the lead-like rule, CMC, WDI and MDDR, on a single platform that is a pre-ADMET web tool. The NCI screened compounds were found to have drug likeness as per the MDDR like rule, and zero violations were observed (Table S-XIV of the Supplementary material).

## CONCLUSION

The compounds (NCI613391, NCI169676, NCI281246 and NCI339580) were identified from NCI database screening based on their close binding interaction with CDK-7 kinase active site residues and then processed for ADMET evaluation. The best compound (NCI613391) was further examined for their capacity to maintain the stability of receptors and receptor-ligand complexes across a 200 ns molecular dynamics simulation. The *RMSD* value of receptor and receptor–ligand complexes was calculated, and it showed that the compounds were found to be stable and remained stable throughout the simulation study. The parallel *RMSF* and gyration radius values of the unbound receptor and backbone atoms of the receptor-ligand complex suggest that the drug molecules inside the CDK7 kinase receptor are also stable. All the compounds were qualified and observed suitable as drug likeness according to the Lipinski rule, Ghose filter, MDDR-like rule and CMC-like rule. Except for NCI169676 and NCI196464, all the compounds were discovered to be CYP450 2D6 substrates, weak substrates for CYP450 3A4 and non-inhibitors of p-glycoprotein. The MM-GBSA and ADMET values of compounds were also displayed in the favourable range, but compound (NCI169676) observed to possess excellent drug likeness (3.54), drug score (0.24), human intestinal absorption (95.36 %) and also displayed a negative AMES and T.E.S.T. toxicity test compared to other compounds with green colour indication. The compound (NCI613391) was found to be a powerful and effective inhibitor of CDK7 kinase and may be further investigated in clinical trials to study its efficacy.

## SUPPLEMENTARY MATERIAL

Additional data and information are available electronically at the pages of journal website: <https://www.shd-pub.org.rs/index.php/JSCS/article/view/12455>, or from the corresponding author on request.

*Acknowledgment.* This project was supported by the Scientific Research Centre at Buraydah Private Colleges under the research project (BPC-SRC/2022-001).

ИЗВОД  
СКОРАШЊА ТАКТИКА ПРЕТРАЖИВАЊА ИНХИБИТОРА CDK-7 КИНАЗЕ  
СКРИНИНГОМ NCI БАЗЕ ПОДАТАКА

MOHAMMAD RASHID<sup>1</sup>, MD TANWIR ATHAR<sup>1</sup>, AFZAL HUSSAIN<sup>2</sup>, NORAH M. ALMADANI<sup>3</sup> и ASHFAQ HUSSAIN<sup>4</sup>

<sup>1</sup>Department of Pharmacognosy and Pharmaceutical Chemistry, College of Dentistry and Pharmacy, Buraydah Private Colleges, Buraydah-51418, Saudi Arabia, <sup>2</sup>Department of Bioinformatics, Maulana Azad National Institute of Technology Bhopal, Madhya Pradesh-462003, India, <sup>3</sup>Biochemistry Department, Faculty of Science, University of Tabuk, Tabuk-47914, Saudi Arabia и <sup>4</sup>Department of Electronics Engineering, Rajasthan Technical University, Kota-324010, India

Ова студија се заснива на претраживању NCI базе података за налажење специфичног инхибитора CDK-7 киназе помоћу HTVS, SP, XP, молекулског докинга, симулације молекулске динамике и процењивањем ADMET. Најбољи инхибитори CDK-7 кин-

азе (NCI613391, NCI169676, NCI281246, NCI339580) су идентификовани скринингом NCI базе података. Стабилност везивне интеракције између рецепторског протеина и протеин-лиганд комплекса нађеног потентног једињења (NCI613391) даље је потврђена симулацијом динамике и MM-GBSA. Вредност RMSD рецептора и рецептор-лиганд комплекса је анализирана, и показала је стабилност везивних интеракција која остаје постојана током симулације. Нађено је да су вредности RMSF и радијус гирације невезаног рецептора и атома основног ланца комплекса једнаки, што указује да је молекул лека унутар CDK7 рецептора такође стабилан. Проучавање MM-GBSA података такође открива јаче везивне интеракције лиганада са CDK7 рецепторима. Са изузетком NCI169676, за сва једињења се показало да су супстрати за CYP 450 2D6, CYP 450 3A4, да су инхибитори за CYP 450 2C9, и нон-инхибитори р-гликопротеина. Сва једињења су била квалификована и погодна као лековима слична, на бази правила Липинског, Ghose филтера, правила MDDR сличности, и правила CMC сличности. Једињење (NCI613391) је испољило апсорпцију у човечкој утроби (76,08 %), и показује негативне Ames и T.E.S.T (US-EPA) токсичности са OSIRIS Property, а нађено је да је обећавајући инхибитор CDK-7 киназе, док његова ефикасност може даље да се испита у клиничким трајалима.

(Примљено 26. јуна, ревидирано 9. августа, прихваћено 21. октобра 2023)

#### REFERENCES

1. L. Kolloch, T. Kreinest, M. Meisterernst, A. Oeckinghaus, *Int. J. Mol. Sci.* **23** (2022) 812 (<http://dx.doi.org/10.3390/ijms23020812>)
2. P. Hazel, S. H. Kroll, A. Bondke, M. Barbazanges, H. Patel, M. J. Fuchter, R. C. Coombes, S. Ali, A. G. Barrett, P. S. Freemont, *Chem. Med. Chem.* **13** (2018) 207 (<http://dx.doi.org/10.1002/cmde.201700826>)
3. M. E. Noble, J. A. Endicott, L. N. Johnson, *Science* **303** (2004) 1800 (<http://dx.doi.org/10.1126/science.1095920>)
4. S. Larochelle, J. Chen, R. Knights, J. Pandur, P. Morcillo, H. Erdjument-Bromage, P. Tempst, B. Suter, R. P. Fisher, *The EMBO J.* **20** (2001) 3749 (<http://dx.doi.org/10.1093/emboj/20.14.3749>)
5. X. Li, D. C. Dean, J. Yuan, T. H. Temple, J. C. Trent, A. E. Rosenberg, S. Yu, F. J. Hornicek, Z. Duan, *Biomed. Pharmacother.* **149** (2022) 112888 (<http://dx.doi.org/10.1016/j.bioph.2022.112888>)
6. G. Lolli, L.N. Johnson, *Cell Cycle* **4** (2005) 565 (<https://pubmed.ncbi.nlm.nih.gov/15876871/>)
7. E. Chipumuro, E. Marco, C. L. Christensen, N. Kwiatkowski, T. Zhang, C. M. Hatheway, B. J. Abraham, B. Sharma, C. Yeung, A. Altabef, *Cell* **159** (2014) 1126 (<http://dx.doi.org/10.1016/j.cell.2014.10.024>)
8. Q. Li, S. Pan, T. Xie, H. Liu, *Blood Sci.* **3** (2021) 65 (<http://dx.doi.org/10.1097/BS9.0000000000000073>)
9. X. Barril, F. Javier Luque, *J. Comput. Aided Mol. Des.* **26** (2012) 81 (<http://dx.doi.org/10.1007/s10822-011-9506-1>)
10. F. Godschalk, S. Genheden, P. Söderhjelm, U. Ryde, *Phys. Chem. Chem. Phys.* **15** (2013) 7731 (<http://dx.doi.org/10.1039/c3cp00116d>)
11. G. Madhavi Sastry, M. Adzhigirey, T. Day, R. Annabhimoju, W. Sherman, *J. Comput. Aided Mol. Des.* **27** (2013) 221 (<http://dx.doi.org/10.1007/s10822-013-9644-8>)

12. *Schrödinger Preparation Wizard*, Lig prep. version 2.6, Glide version 5.8 (2012) ([http://gohom.win/ManualHom/Schrodinger/Schrodinger\\_2012\\_docs/glide/glide\\_quick\\_start.pdf](http://gohom.win/ManualHom/Schrodinger/Schrodinger_2012_docs/glide/glide_quick_start.pdf))
13. A. Hussain, C. K. Verma, *Biomed. Res.* **28** (2017) 5805 (<https://www.alliedacademies.org/articles/molecular-docking-and-in-silico-admet-study-reveals-354aminomethyl-piperidin1yl-methyl1hindol2yl1hindazole6carbonitrile-as-a-potent.pdf>)
14. A. Hussain, C. K. Verma, *J. Cancer. Res. Ther.* **15** (2019) 1131 ([http://dx.doi.org/10.4103/jcrt.JCRT\\_47\\_18](http://dx.doi.org/10.4103/jcrt.JCRT_47_18))
15. QikProp version 4.4 (2010), Schrödinger, LLC, New York, NY, 2015 ([http://gohom.win/ManualHom/Schrodinger/Schrodinger\\_2015-2\\_docs/qikprop/qikprop\\_user\\_manual.pdf](http://gohom.win/ManualHom/Schrodinger/Schrodinger_2015-2_docs/qikprop/qikprop_user_manual.pdf))
16. S. V. Pattar, S. A. Adhoni, C. M. Kamanavalli, S. S. Kumbar, *Beni-Suef Univ. J. Basic Appl. Sci.* **9** (2020) 36 (<https://doi.org/10.1186/s43088-020-00059-7>)
17. A. Hussain, C.K. Verma, U. Chouhan, *Saudi J. Biol. Sci.* **24** (2017) 1229 (<http://dx.doi.org/10.1016/j.sjbs.2015.10.003>)
18. V. Kumar, S. Parate, G. Thakur, G. Lee, H.-S. Ro, Y. Kim, H.J. Kim, M. O. Kim, K. W. Lee, *Biomedicines* **9** (2021) 1197 (<http://dx.doi.org/10.3390/biomedicines9091197>)
19. P. V. Rusina, I. Y. Titov, M. V. Panova, V. S. Stroylov, Y. R. Abdyusheva, E. Y. Murlatova, I. V. Svitanko, F. N. Novikov, *Mendeleev Commun.* **30** (2020) 430 (<http://dx.doi.org/10.1016/j.mencom.2020.07.008>)
20. C. A. Lipinski, F. Lombardo, B. W. Dominy, P. J. Feeney, *Adv. Drug Deliv. Rev.* **23** (1997) 3 ([http://dx.doi.org/10.1016/s0169-409x\(00\)00129-0](http://dx.doi.org/10.1016/s0169-409x(00)00129-0))
21. P. Ertl, B. Rohde, P. Selzer, *J. Med. Chem.* **43** (2000) 3714 (<http://dx.doi.org/10.1021/jm000942e>)
22. A. K. Ghose, V. N. Viswanadhan, J. J. Wendoloski, *J. Comb. Chem.* **1** (1999) 55 (<http://dx.doi.org/10.1021/cc9800071>)
23. T. I. Oprea, *J. Comput. Aided Mol. Des.* **14** (2000) 251 (<http://dx.doi.org/10.1023/a:1008130001697>)
24. A. Kulkarni, Y. Han, A. J. Hopfinger, *J. Chem. Inf. Comput. Sci.* **42** (2002) 331 (<http://dx.doi.org/10.1021/ci010108d>)
25. M. Rashid, *Bioorg. Chem.* **96** (2020) 103576 (<http://dx.doi.org/10.1016/j.bioorg.2020.103576>)
26. S. Kumar, F. Abbas, I. Ali, M. K. Gupta, S. Kumar, M. Garg, D. Kumar, *Phytomed Plus* **3** (2023) 100419 (<https://doi.org/10.1016/j.phyplu.2023.100419>)
27. M. Rashid, O. Afzal, A. S. A. Altamimi, *J. Chil. Chem. Soc.* **66** (2021) 5164 (<http://dx.doi.org/10.4067/S0717-97072021000205164>)
28. S. Thomas, *Explorer, OSIRIS Property*, Actelion Pharmaceuticals Ltd., Allschwil, 2001 (<https://www.organic-chemistry.org/prog/peo/>)
29. T. Martin, *Toxicity estimation software tool (TEST)*, US Environmental Protection Agency, Washington DC, 2016 (<https://www.epa.gov/sites/default/files/2016-05/documents/600r16058.pdf>)
30. N. Sripriya, M. R. Kumar, N. A. Karthick, S. Bhuvaneswari, N. K. U. Prakash, *Drug Chem. Toxicol.* **44** (2019) 480 (<http://dx.doi.org/10.1080/01480545.2019.1614023>)
31. F. S. Prasetiya, W. Destiarani, I. R. C. Prihastaningtyas, M. U. K. Agung, M. Yusuf, *J. Appl. Pharm. Sci.* **13** (2023) 068 (<http://dx.doi.org/10.7324/JAPS.2023.10012>)
32. B. N. Ames, E. Gurney, J. A. Miller, H. Bartsch, *Proc. Natl. Acad. Sci. USA* **69** (1972) 3128 (<http://dx.doi.org/10.1073/pnas.69.11.3128>)

33. P. J. Eddershaw, M. Dickins, *Pharm. Sci. Technol. Today* **2** (1999) 13  
([http://dx.doi.org/10.1016/s1461-5347\(98\)00108-4](http://dx.doi.org/10.1016/s1461-5347(98)00108-4))
34. J. H. Lin, M. Yamazaki, *Clin. Pharmacokinet.* **42** (2003) 59  
(<http://dx.doi.org/10.2165/00003088-200342010-00003>)
35. G. Lolli, E. D. Lowe, N. R. Brown, L. N. Johnson, *Structure* **12** (2004) 2067  
(<http://dx.doi.org/10.1016/j.str.2004.08.013>).